Applied Catalysis B: Environmental 129 (2013) 264–272

Contents lists available at SciVerse ScienceDirect

Applied Catalysis B: Environmental

journal homepage: www.elsevier.com/locate/apcatb

New insight about orange II elimination by characterization of spent activated carbon/Fe Fenton-like catalysts

Filipa Duarte[a], Francisco J. Maldonado-Hódar[b,*], Luis M. Madeira[a]

[a] LEPAE, Department of Chemical Engineering, Faculty of Engineering – University of Porto, Rua Dr. Roberto Frias, s/n, 4200-465 Porto, Portugal
[b] Department of Inorganic Chemistry, Faculty of Sciences – University of Granada, 18071 Granada, Spain

ARTICLE INFO

Article history:
Received 12 July 2012
Received in revised form
18 September 2012
Accepted 21 September 2012
Available online 27 September 2012

Keywords:
Heterogeneous Fenton
Activated carbon
Spent catalyst
TPD
TG

ABSTRACT

This work is focused on the characterization of heterogeneous Fe-based catalysts supported on activated carbons (ACs) that are used in elimination of the azo-dye orange II (OII) from an aqueous solution. The main goal is to clarify the process of OII removal by analyzing textural and chemical surface properties of the fresh and spent activated carbon and Fenton-like catalysts upon using as adsorbents and/or catalysts. Textural changes were analyzed based on the corresponding N_2 adsorption isotherms and the nature of the adsorbed products by TG-DTG and TPD. It was found that OII was adsorbed filling the microporosity without degradation, although interactions between OII molecules and the AC surface groups have been detected. The total organic carbon (TOC) removal is complete in adsorption experiments. In the catalytic experiments using different H_2O_2 concentrations (in the range 6–24 mM) the TOC elimination was never complete and got worse when increasing the H_2O_2 load. The OII molecules were partially oxidized and the adsorption of these products also leads to some blockage of the porosity; higher blockage and higher TOC removals was noticed after experiments carried out with low H_2O_2 concentration. The different TOC removal was related to the interactions of the oxidation products with the carbon surface. When using the highest concentration of the oxidant (24 mM), the highest biodegradability and the lowest toxicity of the treated solution were reached, corroborating again the different nature of the oxidation by-products formed in each case.

1. Introduction

The control of the gaseous and aqueous effluent's quality is today a main priority in order to preserve the environment for future generations. Mainly, the limited water resources in large areas of the world led to the development of water recycling and reuse technologies, which are important from the social, environmental and economic points of view. The nature of the recalcitrant pollutants present in water is quite variable, and they are mainly associated to the different human activities: detergents or drugs in residual urban water, herbicides or pesticides from agriculture, spill of fuel during transport or storage, and many and variable industrial wastes. Special mention should be made to the textile industry, where dyes are extensively used, generating a large amount of polluted water. Dyes are in general poorly biodegradable or even non-biodegradable [1]. Two approaches for dyes elimination are adsorption on porous media or oxidation by using advanced oxidation processes (AOPs) [2–4]. However, adsorption (as well as other physical processes) simply leads to transfer of the pollutants from one phase to another, rather than destroying them.

Among the different AOPs, Fenton reactions present some advantages as simplicity, efficiency and low investment cost, running under mild conditions of temperature and pressure [5]. However, when using homogeneous Fe-catalyzed processes, Fe-ions should be removed from the treated solution to avoid pollution by the metal, which implies the introduction of an extra stage in the treatment, increasing the costs. The development of heterogeneous catalysts is an interesting alternative, avoiding these treatments and favoring the reuse of the catalysts in consecutive batch cycles or in a continuous reactor. The knowledge of the different factors influencing the dye removal when using heterogeneous catalysts can help the optimization of their properties, maximizing their performance and minimizing deactivation and Fe-leaching. Such factors include adsorption and catalysis, co-existent phenomena in this heterogeneous AOP. In both, apart from other properties (like the textural ones), the surface chemistry of the activated carbon/catalyst support and the nature of the parent molecule or oxidation products determine the performance reached in their removal from water. Moreover, the properties of the catalyst, which change during the adsorption/reaction, also play an important role. Such study is the main goal of the current work.

* Corresponding author. Tel.: +34 958 240 444; fax: +34 958 248 526.
E-mail address: fjmaldon@ugr.es (F.J. Maldonado-Hódar).

0926-3373/$ – see front matter © 2012 Elsevier B.V. All rights reserved.
http://dx.doi.org/10.1016/j.apcatb.2012.09.037

Nomenclature

AC	activated carbon
AOP	advanced oxidation processes
DTG	differential thermogravimetry
L_0	micropore size (nm)
N	activated carbon support
N–Fe	catalyst (activated support impregnated with iron)
N–Fe-*X* mM	catalyst used with *X* mM of H_2O_2
N-sat	activated carbon support after one cycle of adsorption (nearly saturated)
OII	orange II
S_{BET}	Brunauer–Emmett–Teller surface area ($m^2\ g^{-1}$)
S_{mic}	microporous surface
TG	thermogravimetry
TOC	total organic carbon (mg_C/L)
TPD	temperature programmed desorption
WL	weight loss (%)
W_0	micropore volume ($cm^3\ g^{-1}$)
XRD	X-ray diffraction

In previous works the authors have developed different heterogeneous Fenton-like catalysts on the basis of different carbon materials (activated carbons (AC) and carbon aerogels (CA)) and different metals (Fe, Co, Ni, Cu). It was shown that the commercial AC Norit RX 3 Extra has the suitable textural properties for this application [6] and, moreover, it was found that iron provides the more active catalyst [7]. The referred commercial AC was chosen to the detriment of aerogels because, in spite of offering high levels of purity, the latter are more expensive materials.

The objective of the present work is to study the elimination of the azo dye Orange II (OII) by adsorption or by catalytic Fenton reaction using AC or Fe/AC heterogeneous catalysts. The performances of each water purification method and the influence of some experimental conditions (as the H_2O_2 concentration) are presented. Special attention is given to the characterization of spent samples and their physical and chemical transformation with the OII elimination process. The correlation of the removal performances with the variation of porous and chemical characteristics of samples is presented, looking for information about the OII elimination in adsorption or catalytic processes. The toxicity/biodegradability of the effluents obtained is also discussed.

2. Material and methods

2.1. Catalysts and supports preparation and characterization

Norit RX 3 Extra (herein called sample N), commercialized as extruded pellets of approximately 3 mm × 5 mm, was milled and sieved to get particles in the powder form (<0.15 mm) and used without additional treatment; with this particle dimensions internal resistances to mass transfer are eliminated [8]. Catalysts were prepared by impregnation with the right amount of iron (II) acetate aqueous solution to obtain a 7 wt.% of iron loading, and finally treated in an inert atmosphere at 300 °C for 2 h for the iron precursor's decomposition.

N_2 (at 77 K) adsorption was applied for the textural characterization of the materials, using a Quantachrome Autosorb-1 apparatus. By applying the Dubinin-Raduskevich [9] and the Stoeckli [10] equation's, the micropore volume, W_0, the mean micropore size, L_0, and the microporous surface, S_{mic}, were obtained. The Brunauer–Emmett–Teller (BET) surface area (S_{BET}) was also obtained from the N_2 adsorption isotherms. Further details can be found elsewhere [6,7].

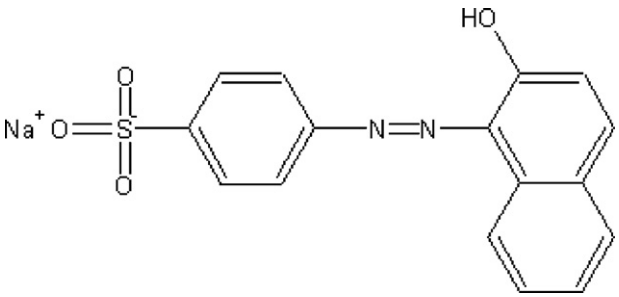

Fig. 1. Orange II molecule.

The chemical characteristics of fresh and used samples was characterized by temperature programmed desorption (TPD) and thermogravimetric analysis (TG-DTG). TPD experiments were carried out by heating the samples to 1000 °C in He flow (60 $cm^3\ min^{-1}$ – atmospheric conditions of temperature and pressure) with a heating rate of 50 °C min^{-1}. The amount of evolved gases was recorded as a function of temperature using a quadrupole mass spectrometer (Balzers, model Thermocube). The oxygen content was calculated from the amounts of CO and CO_2 released during the TPD experiments. TG experiments were performed in He flow (30 $cm^3\ min^{-1}$ – atmospheric conditions of temperature and pressure) and a heating rate of 20 °C min^{-1} using a thermobalance model TGA-50H.

2.2. Catalytic experiments

Tests were carried out in a slurry batch reactor, being the azo dye Orange II (OII) the target model molecule. The chemical structure of the pollutant is shown in Fig. 1.

All experiments were carried out with 1 L of a 0.1 mM OII aqueous solution, using 0.1 g of solid at 30 °C and pH = 3, the reference conditions for the Fenton reaction employed in other works [6,7,11]. The batch reactor was provided with a thermostatic bath (from Huber) to keep the temperature constant along the runs, and magnetic stirring. The initial pH = 3 was set by using a 1 M sulphuric acid solution and remained nearly constant along the catalytic experiments (±0.1). The time zero of the experiments was coincident with the addition of the activated carbon (for adsorption) or the solid + hydrogen peroxide (for catalysis). OII concentration in the experiments was continuously followed by visible spectrophotometry, as detailed in Section 2.3, with the help of a flow-through cell and a peristaltic pump. This parameter, as well as the temperature and pH, were recorded, monitored and saved along the reaction time using a Labview 9.0 interface.

For the assessment of the performance of the support in a second cycle of adsorption, the AC was recovered by filtration of the solution after the first cycle of adsorption (24 h) and reused under the same operating conditions. After all the experiments, the solid adsorbent or catalysts were recovered by filtration and analyzed as previously described.

2.3. Analytical techniques

OII concentration was determined by measuring the absorbance of the solution at 486 nm (characteristic wavelength of the Orange II molecule) using a Philips PU8625 UV/VIS spectrophotometer.

In order to evaluate the mineralization degree, total organic carbon (TOC) analyses were carried out. For that, four samples of 10 ml each were taken and filtered (Reeve Angel microfiber glass filter paper with pores' diameter of 0.8 μm was used) along the catalytic tests. Sodium sulphite in excess was added to the samples (which were kept in the fridge) to guarantee the stop of the reaction, since this reagent consumes instantaneously the residual

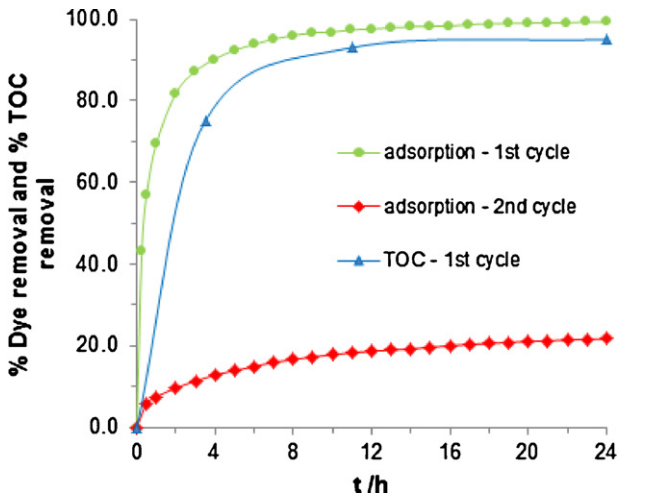

Fig. 2. OII removal in the first and second cycles of adsorption on the AC surface and TOC removal along the first cycle of adsorption (C_{OII} = 0.1 mM, C_{AC} = 0.1 g L^{-1}, T = 30 °C, pH = 3).

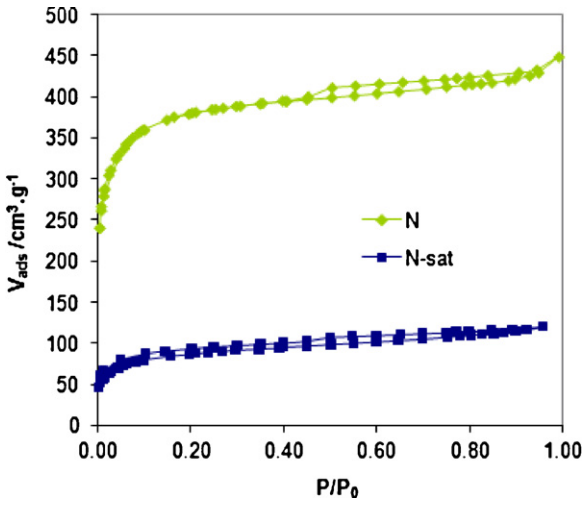

Fig. 3. N_2 adsorption/desorption isotherms of the AC fresh support (N) and the same sample after the first cycle of saturation with OII (N-sat).

hydrogen peroxide. TOC analyses were done in a TOC-500A apparatus. The samples taken were also analyzed by atomic absorption (using a UNICAM 939/959 spectrophotometer) to determine the iron concentration in solution leached from the AC support.

The biodegradability of the treated solutions (after 24 h of reaction) was assessed by respirometry following the O_2 decay along time, in a YSI model 5300 Biological Oxygen Monitor, by comparing the oxygen consumption rate of the sample with that of a standard (sodium acetate) – linear decay along time was observed in both cases. So, two parallel experiments were carried out to determine such consumption rates (k), in both cases using biomass obtained in a WWT activated sludge reactor that treats domestic and textile effluents: (i) 1 ml biomass + 5 ml sample (k_{sample}); (ii) 5 ml distilled water + 1 ml biomass + sodium acetate at the right concentration to get the same TOC as the sample ($k_{sodium\ acetate\ 1}$). The biodegradability (expressed in percentage) of the sample was calculated according to Eq. (1) [12,13]:

$$\%\,\text{biodegradability} = \frac{k_{sample}}{k_{sodium\ acetate\ 1}} \times 100 \quad (1)$$

It is worth noting that the k parameters above-mentioned refer to the values after subtracting the k value from endogenous respiration. For the toxicity evaluation, the solution obtained after protocol (i) was aerated to restore initial dissolved oxygen level, fed with sodium acetate (again at the right concentration to get the same TOC as the sample) and $k_{sodium\ acetate\ 2}$ was obtained similarly. Then, Eq. (2) was applied [12,13]:

$$\%\,\text{toxicity} = \frac{k_{sodium\ acetate\ 1} - k_{sodium\ acetate\ 2}}{k_{sodium\ acetate\ 1}} \quad (2)$$

3. Results and discussion

3.1. Adsorption on the AC support and characterization of the spent material

In a first approach, the behavior of the AC support as adsorbent was studied. The reason behind this is that in heterogeneous Fenton oxidation both phenomena (adsorption and catalysis) coexist; so, adsorption was firstly investigated in the carbon support. The results of the OII elimination in terms of discoloration (followed by absorbance) are illustrated in Fig. 2 for two consecutive adsorption cycles, which showed that the AC adsorption capacity is nearly saturated after the first adsorption cycle. Thus, the AC support used in a single cycle as adsorbent will be called N-sat henceforward, meaning that its surface is almost completely saturated by dye molecules. TOC analysis were also done during the first cycle and revealed a similar tendency as described for the discoloration curve, i.e., almost total TOC removal was achieved by OII adsorption in these experimental conditions (slight differences are due to analytical uncertainties, which are more evident at low TOC levels); decolorization and TOC removal seem to be therefore produced simultaneously by the same phenomenon (adsorption).

To analyze the textural consequences of the support saturation, the N_2 adsorption isotherms were determined (Fig. 3) for fresh and saturated samples, being noteworthy the strong decrease of the adsorption capacity. The BET surface area, micropore volume (W_0, computed by applying the Dubinin-Radushkevich equation) and micropore width (L_0) obtained from the isotherms analysis are shown in Table 1. It was observed a BET surface area decrease from 1405 to 317 m^2 g^{-1} after the first cycle of adsorption. On the other hand, the blockage of the micropore volume allows inferring that the OII adsorption took place mainly into the narrowest micropores, pointed out also by the increase of the L_0 values.

Samples of fresh and saturated AC were analyzed by TG-DTG and the results compared with the TG-DTG of pure OII in order to look for information about the nature of the adsorbed products and the interactions between the solid and the dye molecules. The TG-DTG profile of pure OII is shown in Fig. 4. The dye underwent a 63% of weight loss (WL) by heating in inert atmosphere up to 1200 K, with a main decomposition process at 604 K. Moreover, different decomposition processes inducing less important weight losses were observed at different temperatures, namely at around 820 K or 1020 K. This is a relevant result, because after the thermal degradation of OII in these conditions around 40% remained as solid residue.

The same thermal treatment in TG for the fresh AC yielded a WL of 6.5%, while for the sample of AC saturated with OII by adsorption this parameter increased to 16% – Fig. 5a. In the case of fresh AC, the WL is due only to drying and decomposition of oxygenated surface groups. The main DTG peak (Fig. 5b) at low temperature

Table 1
Textural properties of fresh and OII-saturated AC support.

Sample	S_{BET} (m^2 g^{-1})	W_0 (cm^3 g^{-1})	L_0 (nm)
N	1405	0.62	1.70
N-sat	317	0.14	2.13

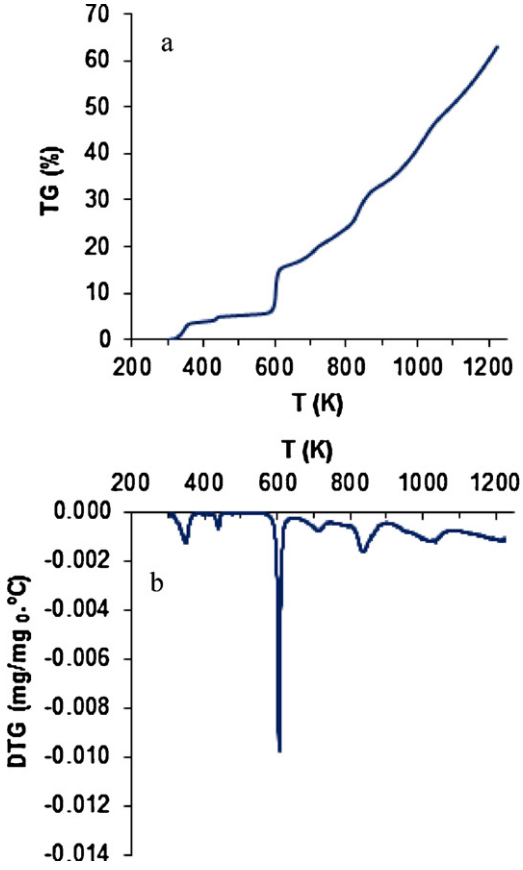

Fig. 4. TG (a) and DTG (b) profiles of pure OII.

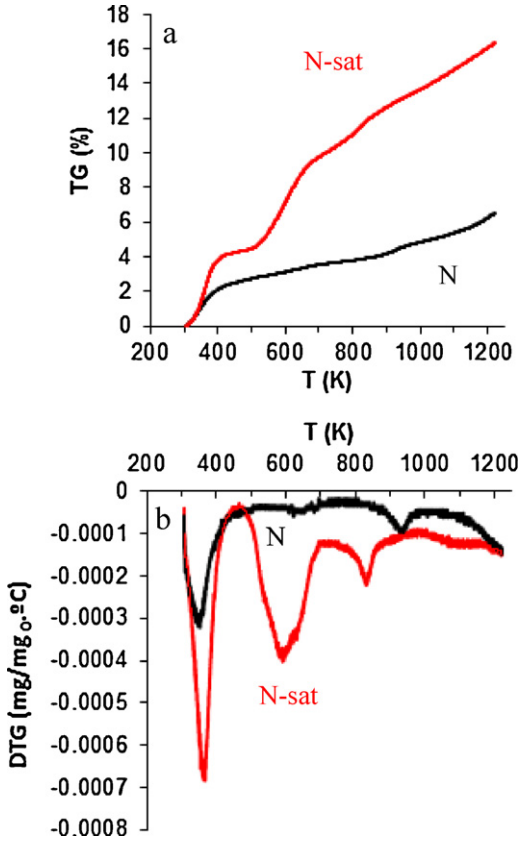

Fig. 5. TG (a) and DTG (b) profiles of fresh AC support (N) and after saturation with OII (N-sat).

Table 2
Oxygen content of fresh and saturated AC support obtained by TPD experiments.

Sample	O (wt.%)	CO μmol g $^{-1}$	CO_2 μmol g $^{-1}$
N	1.8	455	346
N-sat	3.6	1640	307

(around 373 K) was associated with the removal of physisorbed water, although this assumption can mask also certain thermal dehydration of the OII molecule in the saturated sample (according to Fig. 4). Clearly, the other two peaks only existing on the DTG profile of N-sat at around 600 and 820 K correspond to the decomposition of the adsorbed compound. One should note that the decomposition of adsorbed molecules took place at similar temperatures as for pure OII (cf. Fig. 4b). These results, together with the similar evolution of the OII elimination curves determined by discoloration or TOC values, suggest that OII is adsorbed directly without any degradation, filling the micropores of the AC and leading to the observed S_{BET} decrease.

Temperature programmed desorption (TPD) is one of the most powerful and extensively used techniques for the characterization of surface groups in carbon materials [14,15]. The nature and amount of these surface groups can be quantified, which was done by integration of the TPD areas. Thus, this information complements the results obtained from the TG-DTG experiments. The TPD profiles of hydrogen, water, CO and CO_2 evolving from fresh and saturated AC are shown in Fig. 6, while the oxygen content, calculated from the amount of CO and CO_2 evolved, is compiled in Table 2. The total oxygen content increased from 1.8 to 3.6% after the OII adsorption, changing also significantly the corresponding TPD profiles. This increase is mainly due to the higher CO desorption from the N-sat sample, obviously produced by decomposition of the adsorbed dye molecules (Table 2 and Fig. 6).

The oxygen content of the fresh sample is low, according to the nature of untreated ACs. The different oxygenated surface groups were evolved as CO or CO_2 while increasing the temperature. The assignation of the peaks to the different types of surface groups was carried out according to the bibliography. Regarding fresh AC, the CO_2 evolution took place mainly in two temperature intervals: between 300–800 and 800–1100 K, and in both ranges, the CO_2 profiles presented two maxima, located in the first temperature range at 600 and 700 K and at 900 and 950 K in the second temperature interval. The CO profile presented the maximum desorption rate at 1213 K, although one smaller peak at around 550 and a clear shoulder at 950 K are coincident with those previously described for CO_2. In the case of the N-saturated sample, it is evident that the CO_2 evolving peak at 850 K was clearly favored regarding those appearing at lower temperatures, as compared to the N sample. However, the contrary behavior was observed for CO, where the maximum desorption rate shifted to lower temperature, occurring in this case at 600 K vs. 1213 K in the N-sample. The water desorption profile is clearly associated to the decomposition of the new oxygenated surface groups, showing maxima simultaneously to those observed for CO and CO_2 (550 and 850 K), in both cases. Finally, the H_2 evolution started at 900 K while in the fresh sample this occurred only at 1100 K. These changes are therefore due to the thermal decomposition of adsorbed molecules.

These variations were quantified and summarized in Table 2. As commented, after saturation with OII there was a strong increase in the amount of CO desorbed, while the CO_2 slightly decreased. Because the adsorption experiments were carried out in the absence of any additional oxidant, these variations should be associated only with the decomposition of adsorbed species. Three processes are susceptible to contribute to this behavior: (i) the decomposition of the phenol/carbonyl groups of the dye molecule, (ii) the reduction of SO_2 evolved by the carbon matrix, forming CO-

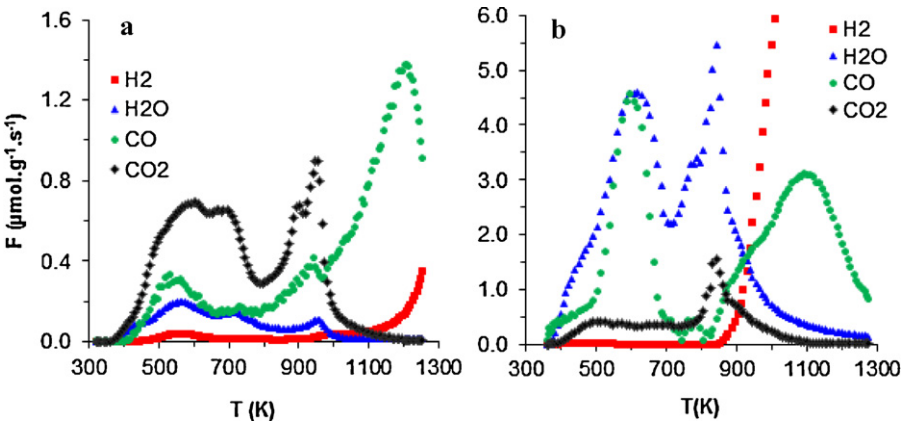

Fig. 6. TPD profiles of (a) fresh AC support and (b) AC after saturation with OII (N-sat).

evolving groups, and (iii), some CO_2 evolving groups (e.g. carboxylic groups) of the AC surface can interact with the OII dye molecule, favoring a chemical adsorption leading to intermediate oxygenated complexes that also evolved as CO. Either the SO_2 release or the OII chemisorption on the AC surface were suggested by Zhang et al. [16]. Taking into account the amount of adsorbed OII (350 mg/g AC, 35 wt.%), the increase in the oxygen content should be of 6.4% instead 1.8%. This difference is mainly due to the fact that the oxygen content shown in Table 2 is obtained only from the CO and CO_2 evolved during the TPD experiments (e.g. H_2O was not considered).

By comparison of the TPD profiles, it can clearly be seen that the peaks corresponding to the decomposition of the carboxyl groups at around 600 K in the N-sample disappeared from the CO_2-TPD profile of N-sat sample, favoring, however, a strong CO-desorption peak in this temperature range. Simultaneously, the formation of anhydrides is also favored, as denoted by the simultaneous evolution of CO and CO_2 at higher temperature. However, the nature of these anhydrides is also influenced by the presence of the adsorbed species, thus, in the saturated sample the CO_2-TPD peaks appear at lower temperature (850 K vs. 950 K). Similarly, the second maximum for CO-desorption occurred at around 1100 K vs. 1213 K observed in the fresh sample.

These TG–DTPs results clearly showed that the OII molecule is chemisorbed on the AC surface, mainly through the original carboxylic groups present in the fresh AC support. This fact generates the formation of intermediate oxygenated surface complexes that evolve as CO. Thus, the amount of CO evolved increased while the CO_2 decreases. The new complexes formed present a very low thermal stability, being mainly evolved at low temperature (600 K), but also, the original CO_x-evolving groups are clearly destabilized, and both anhydrides (CO_2-TPD maxima) and semiquinone (CO-TPD maxima) shifted to lower temperatures. Thus, the previous modification of the surface chemistry of the support can be appropriate to control this kind of interactions in future works.

3.2. Catalytic behavior and nature of adsorbed products

In spite of the high efficiency of AC as OII adsorbent, this process only transfers the pollutants to the adsorbent. So, the main objective of the authors is to develop heterogeneous catalysts able to oxidize pollutants by a Fenton-like process. Firstly, a blank experiment showed that the H_2O_2, used as oxidant, is not able to eliminate the dye by its own. Then, the catalytic role of the AC surface by itself was checked by different experiments. It was found that the discoloration rate is independent of the presence of H_2O_2 in solution (Fig. 7), indicating that in these experimental conditions adsorption on AC is faster than the catalytic removal. Therefore, to estimate the ability of the carbon surface to activate H_2O_2 for the dye oxidation, the adsorptive component was eliminated by a previous saturation of the AC with OII, and then, a catalytic run was carried out in the same experimental conditions. The results obtained (Fig. 7) showed that the AC surface is clearly active as catalyst.

Iron is the most active and selective metal in Fenton-like reactions [5,7] and the AC used as support in this work (Norit RX 3 Extra) has already demonstrated good characteristics to develop supported catalysts, which were successfully applied in very different processes with environmental (e.g. Refs. [17,18]) or fuel chemistry (e.g. Refs. [19,20]) aims, for instance. The catalytic behavior of N–Fe catalyst toward OII elimination was checked in different experimental conditions, namely increasing the oxidant (H_2O_2) concentrations. Evolution of discoloration and TOC removal using different oxidant dosages is presented in Fig. 8a and b. Leaching levels were also assessed along the experiment with the best TOC removal levels (6 mM of H_2O_2). It was observed an increase of the iron concentration in solution with the reaction time, with values of 0.029, 0.081 and 0.345 ppm after 1, 6 and 24 h. To evaluate the contribution for the color removal of the homogeneous process in this experiment, an additional run was carried out with the iron concentration found in solution after 6 h of reaction (0.081 ppm corresponding to 0.25 ppm of iron acetate), when total discoloration was already achieved in the heterogeneous process and the TOC removal had also nearly stabilized. It is observed that the homogeneous reaction removes ca. 26% of color in 6 h (Fig. 8a), but it is noteworthy that the iron amount used in this

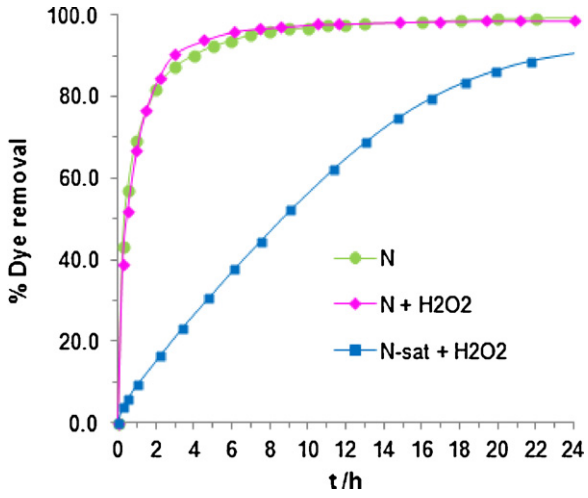

Fig. 7. Comparison of adsorption and catalytic activity of the fresh and OII saturated support (C_{OII} = 0.1 mM, C_{AC} = 0.1 g L^{-1}, $C_{H_2O_2}$ = 6 mM – when used, T = 30 °C, pH = 3).

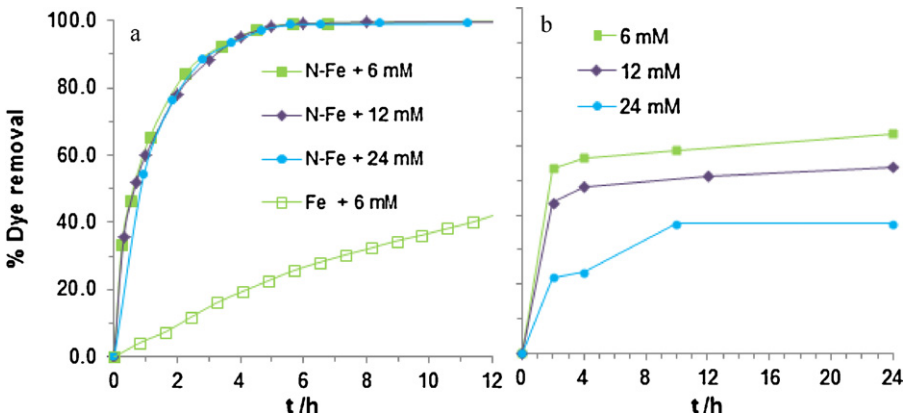

Fig. 8. OII elimination in terms of discoloration (a) and TOC removal (b) using N–Fe/Fe catalysts with different oxidant concentrations (C_{OII} = 0.1 mM, C_{N-Fe} = 0.1 g L^{-1}, C_{Fe} = 0.081 mg L^{-1}, T = 30 °C, pH = 3).

experiment does not correspond to the iron concentration present in solution in the heterogeneous process from the beginning of the reaction. Concerning to the influence of the initial H_2O_2 concentration, it was observed that the dye degradation rate was almost not affected when using H_2O_2 concentrations between 6 and 24 mM (Fig. 8a). The TOC data clearly pointed out that the increase of initial H_2O_2 content is far to improve the mineralization degree, on the contrary, being the TOC removal obtained progressively lower (Fig. 8b). This fact can be due to scavenging reactions (parallel reactions) of the hydroxyl radical due to the presence of excess hydrogen peroxide. The determination of the residual H_2O_2 was carried out by a simple colorimetric method [21] after 24 h of reaction under the conditions of Fig. 8, using the extreme H_2O_2 initial concentrations: 6 and 24 mM. The results showed that in the first case nearly all the oxidant was consumed, while with 24 mM of initial H_2O_2 concentration, the reactant is in excess, and approximately 9 mM remained in solution in spite that around 63% of the initial TOC were not removed (Fig. 8b). Thus, a progressively higher amount of by-products remained in solution, i.e., their nature change with the operational conditions, and/or they are more resistant to the oxidation and were not adsorbed as easily as the dye molecules. Therefore, the solid catalysts were analyzed looking for information about the cause of this behavior.

Analyzing the textural characteristics of the fresh catalyst (Table 3), it is observed a certain decrease of the BET surface area regarding the AC support, because the Fe-phase partially blocked the AC porosity [6,22]. This surface blockage represents only 5% of the total S_{BET} surface, and consequently, cannot justify that by-products were not adsorbed and remained in solution (TOC removal was not complete, as above mentioned). Regarding the used catalysts, it is observed that the decrease of S_{BET} is not as strong as the one observed after adsorption experiments (cf. Tables 1 and 3), and that the evolution of the S_{BET} values is clearly related with the evolution of the TOC removal data (Fig. 8b): the higher TOC removal (corresponding to the use of 6 mM of H_2O_2) yielded the stronger S_{BET} decrease, which induces to think that TOC removal might be also due to a greater adsorption of OII or OII by-products rather than a greater mineralization.

Table 3
Textural parameters of N support, the fresh N–Fe catalyst and the used catalyst samples with 6 and 24 mM of oxidant.

Sample	S_{BET} (m^2 g^{-1})	W_0 (N_2) (cm^3 g^{-1})	L_0 (nm)
N	1405	0.62	1.70
N–Fe	1328	0.58	1.74
N–Fe + 6 mM	577	0.26	1.96
N–Fe + 24 mM	673	0.30	1.90

There are two characteristics of ACs that control their adsorption capacity: the textural properties and the surface chemistry. Obviously, to be adsorbed, the porosity should be accessible to the adsorbate (relation between the pore size of the adsorbent and the adsorbate molecular size), while the surface chemistry controls the interactions between both phases. This last characteristic of the adsorbent is strongly important mainly in adsorption carried out in aqueous solution and was extensively analyzed previously (e.g. Ref. [23]). In our catalytic system, the porosity of the AC support is clearly accessible even to the OII original molecule, because a total elimination of OII by adsorption was detected even by TOC values (cf. Section 3.1). It is expected that the uncolored by-products remaining in solution after the catalytic runs were smaller than the original OII molecule, being therefore also accessible into the AC microporosity. Therefore, chemical interactions should be responsible for this unexpected lower adsorption capacity, which also depends on the oxidation products formed.

Our preliminary studies aiming to identify the intermediate products showed that the primary degradation products might be benzene sulfonate and naftoquinone, i.e., the fractions formed by breakage of the OII molecule by the N=N azo-bond. Also, the main oxidation products detected were benzoic, phtalic and oxalic acids. Nevertheless, the identification of a large amount of additional smaller peaks, the quantification of all the species and the closure of the mass balance, requires a deeper analysis and the application of complementary analytical techniques. Even so, it is worth noting that these results are in agreement with those described in the literature for the OII degradation products, although mainly TiO_2-based catalysts were used for the OII photo-oxidation. According to Stylidi et al. [24], naphthalene-type compounds may be considered as primary degradation products of the dye, originated from oxidative cleavage of the molecule. Several breakdown products of OII including coumarin, 2-naphthol, 2-hydroxy-1,4-naphthoquinone and 1,4-naphthoquinone were identified by GC/MS. From these compounds, a large list of 22 products, progressively smaller and more oxidized, starting by aromatic intermediates containing a six and a five-atom ring, such as phthalic anhydride, were also detected. Bauer et al. [25], by using FT-IR spectroscopy, reveal the presence of C_2 carboxylic aliphatic acids, carbonates and oxygenated sulfur compounds on TiO_2 surfaces. Oxalate, acetate, carbonates and oxygenated sulfur compounds were identified as the final degradation products. The oxidation of Orange II by hydrogen peroxide catalyzed by iron (III) complexes in aqueous solutions at pH 9–11 leads to CO_2, CO, phthalic acid and smaller aliphatic carboxylic acids as major mineralization products [26].

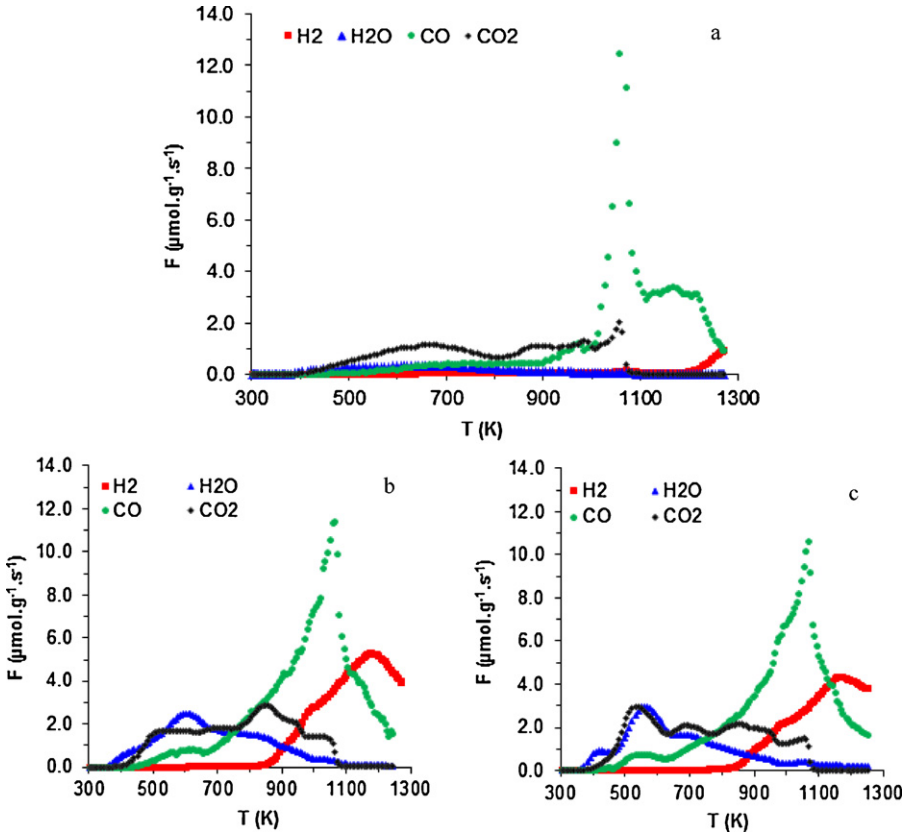

Fig. 9. TPD profiles of fresh (a) and used catalysts with 6 mM (b) and 24 mM (c) of H_2O_2.

Obviously, the degree of mineralization, concentration and ratios of intermediate products, etc. will be strongly influenced either by the catalysts characteristics as by the experimental conditions. So, looking for information about properties of the used catalysts, TPD profiles were obtained for fresh and spent catalysts – Fig. 9 – and the amount of products evolved determined and compiled in Table 4.

Regarding the characterization of fresh catalyst (pretreated at 300 °C = 573 K), it is observed that the TPD profiles are quite similar to those of the original AC support (cf. Fig. 6), except by the strong CO desorption peak observed at 1060 K (Fig. 9). At this temperature, there is simultaneously a small CO_2-desorption peak. The strong CO peak is associated with the reduction of the iron oxide particles (the only difference regarding the support). The calculated oxygen content of the catalyst increased 2.8% regarding the bulk AC (Table 4), which is also in agreement with a Fe-content of 7 wt.% (taking into account that Fe_3O_4 and/or Fe_2O_3 were found to be the principal iron species [6]).

When analyzing the TPD of used catalysts (Fig. 9b and c), the different nature of the adsorbed species regarding spent samples used as adsorbents (Fig. 6b) is observed at a glance. Thus, the TPD profiles of used catalyst also present a main CO peak associated to iron oxides reduction. Nevertheless, this peak becomes wider regarding fresh samples and clearly involves all the additional decomposition of CO-evolving groups between 700 and 1300 K associated to the decomposition of adsorbed molecules. Also, at low temperatures, where the TPD profile is not influenced by the iron oxides reduction, while in the N-sat sample the main decomposition process occurred at around 560 K, being the CO-desorption preferential regarding the CO_2 one, in the residues of catalysts the CO_2-desorption is preferential in this temperature range, although CO-desorption also occurred. The CO-TPD profile increased more or less homogeneously between 700 and 1060 K, showing small shoulders, and then, decreased similarly. The CO_2-profile showed also clearly the existence of different surface groups by some maxima with variable intensity depending on the experimental conditions used in the catalytic process, i.e., the dose of oxidant. The decay of this profile is coincident with the maximum CO-desorption probably because the iron particles are able to catalyze the oxidation of the carbon surface ($CO_2 + C = 2CO$). The H_2O-profile is also clearly associated to the decomposition of carboxylic acid, in spite that the large tail and small shoulders also justified different processes such as the phenolic group decomposition. The hydrogen desorption of both spent samples showed a maximum located at 1150–1200 K; in this case, the H_2-evolution starts at a similar temperature than in spent adsorbents, but increases with smaller slope and in both cases defines a clear maxima.

In spite of the quite similar oxygen content evaluated for both catalyst residues after processes at low (6 mM) and high (24 mM) H_2O_2 concentrations (Table 4), the formation of carboxylic acid is clearly favored in the later as denoted by the intense peak observed on the CO_2-profile at 530 K with simultaneous H_2O-desorption. In this case, also the amount of CO_2 evolved is slightly higher, indicating a greater oxidation degree of the adsorbed compounds on the AC surface.

Table 4
Oxygen content obtained by TPD of the AC support, and fresh and used N–Fe catalysts with 6 and 24 mM of oxidant.

Sample	% O	CO µmol g^{-1}	CO_2 µmol g^{-1}
N	1.8	455	346
N–Fe	4.6	1566	647
N–Fe + 6 mM	10.6	3514	1550
N–Fe + 24 mM	10.7	3340	1661

Table 5
Parameters of biodegradability and toxicity for the initial poluent solution and for the solution treated by the heterogeneous Fenton process using 6 and 24 mM of H_2O_2.

	Biodegradability (%)	Toxicity (%)
OII initial solution	16	80
N–Fe + 6 mM	65	60
N–Fe + 24 mM	90	34

This fact can clearly influence the adsorption capacity of the by-products formed. The carbon surface is amphoteric, and there is a broad bibliography regarding adsorption of pollutants on ACs as a function of pH, surface chemistry, nature of the organic pollutants, etc. All these parameters determine the attractive or repulsive interactions between both phases in solution. Dispersion (van der Wals) interactions also play an important role, thus, aromatic solutes have a high affinity for graphene layers of the AC favored by π–π interactions. These interactions are weakened by the presence of acidic oxygenated groups on the edge of the graphene layers because serve to withdraw electrons from the π-system deactivating the ring system of AC – e.g. it is well known that the adsorption of phenol is retarded by the acidity of the carbons [27], but also, the aromatic ring of a solute (pollutant) is deactivated depending on the substituents (phenol, chlorophenol, dinitrophenol, etc.) [28]. Thus, increasing the H_2O_2 dose used in reaction, the total mineralization capacity is not increased, probably by the development of scavenging reactions in a greater extent; nevertheless, the by-products formed are clearly more oxidized than those formed at low H_2O_2 concentrations. The greater TOC removal observed in the latter case is therefore a consequence of a greater adsorption of by-products that provoked a greater pore blockage.

In order to check these conclusions, and also looking for some indications about the evolution of the solution biodegradability/toxicity after the different treatments, some additional experiments were carried out. It is noteworthy that the partial oxidation of organic contaminants may lead to more toxic by-products than the initial compounds [29], independently of the TOC decay. Thus, biodegradability and toxicity of the initial and treated solutions (with 6 and 24 mM of H_2O_2) were analyzed and the results proved that the present process led to an increase of effluent biodegradability, as well as to a decrease of the toxicity relatively to the initial dye solution (Table 5). It is observed that the process that used a higher H_2O_2 concentration presented the highest biodegradability and, accordingly, the lowest toxicity. However, it is important to note that the values for these parameters depend on the microorganisms used as well as on the method applied, which should be chosen accordingly to the final destination of the treated water [29]. The biodegradability/toxicity dependence on initial hydrogen peroxide concentration follows a different trend as compared to TOC data. These results confirm the different nature of the by-products generated in each experimental condition, which are in clear agreement with those previously discussed.

4. Conclusions

This work deals with the characterization of used samples after adsorption and catalytic experiments in order to clarify the process implicated in the elimination of OII from an aqueous solution by the heterogeneous Fenton advanced oxidation using a Fe/AC catalyst. It is known that this process involves the coexistence of adsorption and reaction phenomena, so adsorption experiments were firstly carried out; they allowed concluding that the OII molecules are adsorbed without any transformation, although interactions with the surface groups of the AC have been detected by TPD. The main difference detected in the AC after the adsorption was the increase of CO and the decrease of CO_2 desorption amounts, which were attributed to (i) the decomposition of OII molecule groups; (ii) the interaction of these molecules with the CO_2-evolving groups of the AC surface (chemical adsorption); (iii) the reduction of SO_2 that came from AC and/or the OII molecules. Upon adsorption a blockage of the porosity was observed, particularly micropores where dye molecules are retained.

Catalytic runs were done with different oxidant concentrations. The higher TOC removal was obtained with a 6 mM concentration of H_2O_2. However, a significant amount of intermediate products still stayed in solution, i.e., they are not mineralized or adsorbed. Because OII molecules are easily adsorbed, this lack of by-products adsorption is due to chemical interactions that did not favor the affinity between adsorbent–adsorbate, particularly using higher concentrations of H_2O_2 (that also favors the scavenging). The textural and chemical characterization of spent catalysts pointed out that S_{BET} decrease was stronger when using a low H_2O_2 load (6 mM). However, TPD and biodegradability experiments showed that by-products formed at higher H_2O_2 concentrations are more oxidized, which difficult their adsorption, but decreases their toxicity.

Acknowledgements

FD is grateful to the Portuguese Foundation for Science and Technology (FCT) for her PhD grant (ref. SFRH/BD/44703/2008). FJMH acknowledges the Spanish MICINN for CTM2010-18889 and AIB2010PT-00378 projects. FD and LMM are also grateful for funding by the Portugal–Spain cooperation project (Integrated Action with ref. AI-E/11). The authors also acknowledge the precious support of Carmen Rodrigues in the biodegradability/toxicity tests.

References

[1] U. Pagga, D. Brown, Chemosphere 15 (1896) 479–491.
[2] F.M. Saunders, J.P. Gould, C.R. Southerland, Water Research 17 (1983) 1407–1419.
[3] H.Y. Shu, C.R. Huang, M.C. Chang, Chemosphere 29 (1994) 2597–2607.
[4] K. Tanaka, K. Padermpole, T. Hisanaga, Water Research 34 (2000) 327–333.
[5] R.J. Bigda, Chemical Engineering Progress 92 (1995) 62–66.
[6] F. Duarte, F.J. Maldonado-Hódar, L.M. Madeira, Applied Catalysis B 103 (2011) 109–115.
[7] F. Duarte, F.J. Maldonado-Hódar, A.F. Pérez-Cadenas, L.M. Madeira, Applied Catalysis B 85 (2009) 139–147.
[8] F. Duarte, F.J. Maldonado-Hódar, L.M. Madeira, Industrial and Engineering Chemistry Research 51 (2012) 9218–9226.
[9] R.C. Bansal, J.B. Donnet, F. Stoeckli, Active Carbon, Marcel Dekker, New York, 1988.
[10] F. Stoeckli, A. Guillot, A.M. Slasli, D. Hugi-Cleary, Carbon 40 (2002) 211–215.
[11] J.H. Ramirez, F.J. Maldonado-Hódar, A.F. Pérez-Cadenas, C. Moreno-Castilla, C.A. Costa, L.M. Madeira, Applied Catalysis B 75 (2007) 312.
[12] M. Farré, M. Franch, J. Ayllón, J. Peral, X. Domènech, Desalination 211 (2007) 22–33.
[13] R.C. Martins, R.M. Quinta-Ferreira, Chemical Engineering Science 66 (2011) 3243–3250.
[14] J.L. Figueiredo, M.F.R. Pereira, M.M.A. Freitas, J.J.M. Orfão, Carbon 37 (1999) 1379–1389.
[15] S. Morales-Torres, F.J. Maldonado-Hódar, A.F. Pérez-Cadenas, F. Carrasco-Marín, Journal of Hazardous Materials 183 (2010) 814–822.
[16] G. Zhang, J. Qu, H. Liu, A.T. Cooper, R. Wu, Chemosphere 68 (2007) 1058–1066.
[17] I. Mesquita, L.C. Matos, F. Duarte, F.J. Maldonado-Hódar, A. Mendes, L.M. Madeira, Journal of Hazardous Materials 237–238 (2012) 30–37.
[18] J.P.S. Sousa, M.F.R. Pereira, J.L. Figueiredo, Catalysis Today 176 (2011) 383–387.
[19] B. Pawelec, R. Mariscal, J.L.G. Fierro, A. Greewood, P.T. Vasudevan, Applied Catalysis A 206 (2001) 295–307.
[20] S. Echeandia, P.L. Arias, V.L. Barrio, B. Pawelec, J.L.G. Fierro, Applied Catalysis B 101 (2010) 1–12.
[21] R.M. Sellers, Analyst 105 (1990) 950–954.
[22] A. Rey, M. Faraldos, J.A. Casas, J.A. Zazo, A. Bahamonde, J.J. Rodríguez, Applied Catalysis B 86 (2009) 69–77.

[23] L.R. Radovic, C. Moreno-Castilla, J. Rivera-Utrilla, Carbon Materials as Adsorbents in Aqueous Solutions in Chemistry and Physics of Carbon, vol. 27, Marcel Dekker, Inc., New York, 2000, 227–405.
[24] M. Stylidi, D.I. Kondarides, X.E. Verykios, Applied Catalysis B 40 (2003) 271–286.
[25] C. Bauer, P. Jacques, A. Kalt, Journal of Photochemistry and Photobiology 140 (2001) 87–92.
[26] N. Chahbane, D. Popescu, D.A. Mitchell, A. Chanda, D. Lenoir, A.D. Ryabov, K. Schramma, T.J. Collins, Green Chemistry 9 (2007) 49–57.
[27] H. Oda, M. Kishida, C. Yokokawa, Carbon 19 (1981) 243–248.
[28] F. Caturla, J.M. Martín-Martínez, M. Molina-Sabio, F. Rodriguez-Reinoso, R. Torregrosa, Journal of Colloid Interface Science 124 (1988) 528–534.
[29] L. Rizzo, Water Research 45 (2011) 4311–4340.